Chinese Herbal Medicines 15 (2023) 123–131

Contents lists available at ScienceDirect

Chinese Herbal Medicines

journal homepage: www.elsevier.com/locate/chmed

Original Article

Identification of anti-inflammatory components in *Panax ginseng* of Sijunzi Decoction based on spectrum-effect relationship

Hong Kan [a,b], Dongxue Zhang [a], Weijia Chen [a], Shihan Wang [a], Zhongmei He [a], Shifeng Pang [b], Shuai Qu [c,*], Yingping Wang [a,*]

[a] College of Chinese Medicinal Materials, Jilin Agricultural University, Changchun 130118, China
[b] Institute of Special Animal and Plant Sciences of Chinese Academy of Agricultural Sciences, Changchun 130112, China
[c] Jilin Institute of Biology, Changchun 130012, China

ARTICLE INFO

Article history:
Received 22 February 2022
Revised 11 April 2022
Accepted 21 April 2022
Available online 17 October 2022

Keywords:
anti-inflammation
ginsenosides
Panax ginseng C.A. Mey
Sijunzi Decoction
spectrum-effect relationship
ulcerative colitis

ABSTRACT

Objective: This study aimed to identify the main medicinal active components of *Panax ginseng* (*P. ginseng*) in the compatibility environment of clinical application. For this purpose, the anti-inflammatory ingredients of *P. ginseng* were investigated based on its therapeutic effect in Sijunzi Decoction (SJD) which is a widely used traditional Chinese formula.

Methods: The fingerprints of 10 batches of SJD consisting of different sources of *P. ginseng* were established by UPLC technique to investigate the chemical components. At the same time, the anti-inflammatory effects of these components were evaluated by dextran sulfate sodium-induced ulcerative colitis mouse model. Grey relational analysis was applied to explore the correlation degree between fingerprints and anti-inflammatory effects in SJD. Lipopolysaccharide-stimulated RAW264.7 murine macrophages were established to evaluate the anti-inflammatory action of the screened effective substances of *P. ginseng*.

Results: According to grey relational analysis, notoginsenoside R_1, ginsenoside Rg_2 and ginsenoside Rb_3 of *P. ginseng* were the major anti-inflammatory contributions in SJD. They had been proven to be closely associated with the anti-inflammatory process of SJD and displayed a close effect compared with SJD by LPS-stimulated RAW264.7 murine macrophages.

Conclusion: Our work provides a general strategy for exploring the pharmacological ingredients of *P. ginseng* in traditional Chinese formulas which is beneficial for establishing the quality standards of traditional herbs in traditional Chinese medicine prescription based on their clinical therapeutic effect.

1. Introduction

Roots of *Panax ginseng* C. A. Mey are a well-known traditional Chinese medicine (TCM) in China and widely used clinically in traditional Chinese formulas. Ginsenosides are the main active constituents that show various pharmacological effects such as immunoregulation effect (Hao et al., 2019), antioxidant activity (Chen & Huang, 2019), anti-inflammatory, anti-nociceptive effects, etc (Lee et al., 2019; Cao et al., 2021). The growth of *P. ginseng* was affected by plant origin, species, ages, parts, soils or climates, which may lead to the differences of chemical compositions and bioactivities (Liu & Xiao, 1992; Shi, Wang, Li, Zhang, & Ding, 2007; Kang et al., 2008; Li et al., 2012; Shan, Luo, Huang, & Kong, 2014; Zhang et al., 2018). Consequently, it is urgent to investigate the main active components of *P. ginseng* to establish a quality standard ensuring clinical efficacy.

The characteristics of multiple-effects of TCM are conveyed through prescriptions for the specific disease in clinic. Therefore, the orientated effective components of TCM ought to be discovered under the condition of prescription compatibility, which provides an environment for exerting its efficacy. Sijunzi Decoction (SJD) is a classic traditional Chinese formula consisting of *P. ginseng*, *Atractylodes macrocephala* Koidz. *Porica cocos* (Schw.) Wolf and *Glycyrrhiza uralensis* Fisch. (Wang et al. 2013). It has been widely applied in gastrointestinal diseases for thousands of years in China. Previous studies demonstrated that SJD can significantly improve the inflammatory response to colitis (Lu et al., 2017; Song et al., 2016; Yu, Lu, Zhang, Zhang, & Yan, 2016; Gao, Peng, & Li, 2018).

* Corresponding authors.
E-mail addresses: qushuai1027@163.com (S. Qu), yingpingw@126.com (Y. Wang).

https://doi.org/10.1016/j.chmed.2022.04.003
1674-6384/

According to the compatibility theory of TCM, *P. ginseng* is the monarch drug of SJD, which means that *P. ginseng* plays a major therapeutic role in the prescription. Therefore, SJD was regarded as a carrier to study the pharmacodynamic substances of *P. ginseng* in this research.

Chromatographic fingerprint analysis is considered to be an appropriate method to assess the consistency of botanical drugs approved by both the Food and Drug Administration and the European Medicines Agency (Li, Chen, Jia, & Xie, 2013). Therefore, chromatographic fingerprint analysis is a rational approach for quality assessment of traditional Chinese herbal medicine (Xie et al., 2006). However, chemical components are not identical to effective substances. For this reason, a spectrum-effect relationship integrating the chemical fingerprints with pharmacological effects is established to hunt for the functional constituents. It already has extensive use in guaranteeing the quality and ascertaining bioactive ingredients in TCM (Liu, Zhu, Liu, & Zhang, 2019; Zhang et al., 2019; Shen et al. 2018; He & Zhou, 2021).

Grey relational analysis (GRA) can estimate the degree of correlation between the two factors based on the comparison of similarities in the shapes of the various factors, which is often used to reveal quantitative comparisons of trends in dynamically changing systems (Kadier et al., 2015; Nelabhotla, Jayaraman, Asghar, & Das, 2016; Zhou et al., 2016). GRA has several advantages such as a small sample size, a small amount of calculation, and good intuition compared with other analysis methods (Shen et al., 2018).

In this study, GRA was applied to analyze the connection between chemical compositions in the fingerprints of SJD and pharmacodynamics evaluated by the ulcerative colitis (UC) mouse model. It aims to investigate the main activity substances with anti-inflammatory activities of *P. ginseng* in SJD during the process of treating UC. Compared with conventional fingerprints, this research restores *P. ginseng* to the "compatibility environment" of SJD which is coincident with the essential characteristics of the compatibility theory and clinical functions of TCM. Our results showed that notoginsenoside R_1, ginsenoside Rg_2 and ginsenoside Rb_3 were the main activity substances of anti-inflammatory activities of *P. ginseng* in SJD. It can provide a strategy for establishing the quality standards of traditional herbs in traditional Chinese medicine prescription based on their clinical therapeutic effect.

2. Materials and methods

2.1. Chemicals and reagents

Notoginsenoside R_1 (R_1), ginsenoside Rb_1 (Rb_1), ginsenoside Rb_2 (Rb_2), ginsenoside Rb_3 (Rb_3), ginsenoside Rg_1 (Rg_1), ginsenoside Rg_2 (Rg_2), ginsenoside Rf (Rf), ginsenoside Ro (Ro), ginsenoside Rd (Rd), ginsenoside Re (Re), (20*S*)-ginsenoside Rg_3 ((20*S*)-Rg_3), (20*R*)-ginsenoside Rg_3 ((20*R*)-Rg_3), ginsenoside Rk_2 (Rk_2) (≥98% pure) were provided by the Shanghai Yuanye Biotechnology Co., ltd. (Shanghai, China). *P. ginseng*, *A. macrocephala*, *P. cocos* and *G. uralensis* applied in the study were purchased from Fusong Shenyuan Changbaishan Ginseng Technology Co., ltd. (Fusong, China).

Acetonitrile was purchased from Fisher Scientific (Waltham, MA, USA). Water was purified through a Milli-Q water purification system (Millipore, MA, USA). TNF-α, IL-1β, IL-6 and NO ELISA kits were provided by Jiangsu Mai Sha Industry Co., ltd (Yancheng, China). Dextran sulfate sodium (DSS) was obtained from MP Biomedicals (California, USA). Cell Counting Kit-8 (CCK-8) was obtained from Biosharp Life Science (Shanghai, China). Lipopolysaccaride (LPS) was purchased from Sigma-Aldrich (St. Louis, MO, USA). Griess reagents were purchased from Promega (Madison, USA).

2.2. Instruments and conditions

Chromatographic analysis was performed on a Waters ACQUITY UPLC system equipped with a photodiode array detector (Waters, USA).

2.2.1. UPLC conditions

Chromatographic separation was performed on a waters CSH-C_{18} column (2.1 mm × 150 mm, 1.7 μm) and maintained at 35 °C. The detection wavelength was monitored at 203 nm. The flow rate was 0.3 mL/min. The injection volume was 2 μL.

The mobile phase consisted of phosphoric acid aqueous solution (A) and acetonitrile (B) with the following optimized gradient elution: 0–7 min: 17%, 7–9 min: 17%–17.5%, 9–14 min: 17.5%–21%, 14–16 min: 21%–22%, 16–21 min: 22%–23%, 21–24 min: 23%–26%, 24–25 min: 26%–30%, 25–31 min: 30%–32%, 31–35 min: 32%–33%, 35–38 min: 33%–33%, 38–40 min: 33%–50%, 40–43 min: 50%–51%, 43–45 min: 51%–53%, 45–50 min: 53%–60%, 50–53 min: 60%–100%.

2.2.2. Method validation

Five sample solutions of SJD were analyzed to determine the precision. The repeatability was evaluated by five injections of one sample. Stability study of the sample was performed at different times in 0, 2, 4, 6, 12, and 24 h. Each sample solution was detected three times in parallel.

2.3. Preparation of 10 batches of SJD

All the herbs, *P. ginseng, A. macrocephala*, *P. cocos*, and *G. uralensis*, were crushed into powder and mixed in the proportion of 3:3:3:2 according to the composition recorded in "*Taiping Huimin Heji Ju Fang*". Then, the four ingredient herbs with a total weight of 25 g were soaked in ten times the volume of deionized water (250 mL) and reflux extracted twice for 1.5 h, respectively. The merged aqueous solution was evaporated to a concentration of 0.5 g crude drug/mL under reduced pressure. Then, 10 mL aqueous solution was subjected to alcohol precipitation overnight, followed by evaporation of ethanol. The remaining aqueous solution was first extracted with 10 mL of ether and then extracted with 10 mL of water-saturated *n*-butanol three times. The *n*-butanol fraction was evaporated and diluted in 2.5 mL methanol. Then, after being filtered by a 0.22 μm syringe filter, the sample solution with a volume of 2 μL was analyzed by the UPLC system to obtain fingerprints. Individual standards were mixed and dissolved in methanol to obtain ginseng saponin combinations.

Considering the practical application, among the 10 batches of *P. ginseng*, farmland *P. ginseng* is the most widely applied in clinical practice due to its fertility and low cost. Therefore, in this study, SJD made of 5-year-old farmland *P. ginseng* (S10) was regarded as the model SJD generally representing SJD. The above sample solutions were further diluted 10 times to calculate the content of R_1, Rg_2 and Rb_3 in model SJD.

2.4. Anti-inflammation evaluation of SJD

2.4.1. Animal handling and tissue collection

Male BABL/c mice (20–22 g) were provided by Changchun Institute of Biological Products Co., ltd. (Changchun, China). The animals were housed in a 12 h light/dark cycle at the animal center of Institute of Special Animal and Plant Sciences of Chinese Academy of Agricultural Sciences for 7 d before experiments.

All animals were handled in strict accordance with good animal practice according to the Animal Ethics Procedures and Guidelines of the People's Republic of China, and the study was approved by The Animal Administration and Ethics Committee of the Institute

of Special Animal and Plant Sciences, Chinese Academy of Agricultural Sciences (Permit No. ISAPSAEC-2018-001). The mice were randomly separated into 12 experimental groups: control group (n = 10), UC model group (n = 12), 10 different batches of SJD group (S1 – S10, n = 10). The control group was administrated with water. The UC model group and the SJD groups received 3% DSS in drinking water for 6 d. On the fourth day, SJD groups took SJD orally at a dose of 4.5 g crude drug/kg/d for the next 7 d.

Mice were euthanized and sacrificed at the end of experiment. After standing for 30 min, the blood sample was centrifuged at 4 °C (4 000 rpm for 20 min) and stored at – 80 °C for further study. The full-length colon was isolated and rinsed with normal saline. The images of colons in different treatments were collected.

2.4.2. Histological evaluation

The colon tissues of model SJD were fixed with 10% formaldehyde and paraffin embedded for histological evaluation. The colonic specimens (5 μm) were stained with hematoxylin & eosin (H&E) and the histological changes were observed by a light microscope.

2.4.3. Immunohistochemistry (IHC) analysis

Occludin and ZO-1 were detected by IHC staining according to the methods reported before (Guo et al., 2018). The samples of model SJD were incubated with the primary antibodies (occludin and ZO-1) overnight at 4 °C. Biotinylated immunoglobulin cocktail of goat anti-rabbit IgG was then applied at 37 °C for 20 min. DAB kit was used for the chromogenic reaction and the nucleus was then stained with hematoxylin for 1 min. The colon specimens were captured by a microscope at the ×400 magnification.

2.4.4. Cytokine analysis by ELISA

The serum levels of tumor necrosis factor α (TNF-α), interleukin-1β (IL-1β), interleukin-6 (IL-6) and nitric oxide (NO) were determined with ELISA kits following manufacturers' instructions.

2.4.5. NO production assay in vitro

RAW 264.7 macrophages were seeded in 24-well plates at (5.0×10^5)/mL and incubated for 12 h at 37 °C with 5% CO_2. The macrophages were treated with LPS (1 μg/mL) for 30 h in the presence or absence of sample solutions. The concentration of samples in macrophages were determined according to the cell viability detected by a CCK-8 assay reported in the literature (Qiao et al., 2019). After incubation, each culture supernatant (100 μL) was mixed with an equal volume of Griess reagent (1% sulfanilamide and 0.1% naphthylethylenedimine dihydrochloride in 2.5% phosphoric acid). The reaction was maintained for 10 min in the dark. Absorbance was measured at 520 nm in a microplate reader (Biotek Synergy Instrument, Vermont, USA). Nitrite concentrations were calculated using a $NaNO_2$ standard calibration curve.

2.5. Statistical analysis

Statistical analysis was analyzed by GraphPad Prism V7.0. The levels of proinflammatory cytokines TNF-α, IL-1β, IL-6 and NO were presented as mean ± standard deviation (SD). IHC assays were analyzed with one-way analysis of variance (ANOVA) followed by Tukey's test. $P < 0.05$ was considered statistically significant.

2.6. Gray relational analysis

Grey theory is an effective model established by Professor Deng for acquiring uncertain knowledge. It mainly focuses on quantitatively describing and comparing the development tendency of a system. Grey relation degree is the key of GRA, which is obtained by comparing the geometrical similarity between reference data sequence and several comparative data sequences. The higher the grey relation degree, the closer development direction and rate of these sequences, and their relationship will be closer to each other (Dai, Liu, & Hu, 2014).

Steps in GRA include (1) data processing and normalizing and (2) calculating grey relational coefficient. The normalization process is calculated by Eqs. (1) and (2). The grey relational coefficient can be obtained by Eq. (3) from the normalized values. In the middle of the calculation, the coefficient constant is assumed to be ρ = 0.5.

$$X_{i(k)} = \frac{X_i - X_{min}}{X_{max} - X_{min}} \tag{1}$$

$$X_{i(k)} = \frac{X_{max} - X_i}{X_{max} - X_{min}} \tag{2}$$

where Eq. (1) is for the higher the better attributes or criterion; Eq. (2) is used for the smaller the better attributes or criterion. i = 0, 1……, n; k = 1, 2, ……, m.

$$\zeta_i(k) = \frac{\min\limits_i \min\limits_k |X_0(k) - X_i(k)| + \rho \cdot \max\limits_i \max\limits_k |X_0(k) - X_i(k)|}{|X_0(k) - X_i(k)| + \rho \cdot \max\limits_i \max\limits_k |X_0(k) - X_i(k)|} \tag{3}$$

where,

(1) $\min\limits_i \min\limits_k |X_0(k) - X_i(k)|$ is the smallest value of *Xi(k)*;
(2) $\max\limits_i \max\limits_k |X_0(k) - X_i(k)|$ is the largest value of *Xi(k)*;
(3) $|X_0(k) - X_i(k)|$ is the absolute value of the difference between $X_0(k)$ and $X_i(k)$;
(4) ρ is the coefficient constant, which is defined in the range $0 \le \rho \le 1$. In the middle of the calculation, the coefficient constant is assumed to be ρ = 0.5.

3. Results

3.1. Results of UPLC fingerprints

In order to obtain a good resolution among the numerous chemical compounds in Chinese herbal formula, we compared Acquity UPLC CSH C_{18} RP column (150 mm × 2.1 mm, particle size of 1.7 μm) and Acquity UPLC BEH C_{18} RP column (50 mm × 2.1 m m, particle size of 1.7 μm). The CSH column showing better peak-to-peak resolution of the constituents was chosen to separate the compounds in SJD. Moreover, the UV absorption wavelength was set at 203 nm to reduce interference of chemical constituents from other herbs in SJD. Method validation data listed in Table 1 showed the relative standard deviation (RSD) of the precision, repeatability and sample stability which were calculated by the peak area of compounds. The precision and repeatability of the results were both <3% which certified that the chromatographic conditions were suitable. In the sample stability test, RSD of the samples was also <3% which demonstrated the samples were stable in 24 h.

UPLC fingerprints of 10 batches of SJD (S1–S10) made of different resources of *P. ginseng* shown in Fig. 1A were obtained and matched automatically by the Similarity Evaluation System for Chromatographic Fingerprint of Traditional Chinese Medicine, which was devised by the Chinese Pharmacopoeia Committee (Version 2012A) (Beijing, China). A representative reference fingerprint was formed automatically by the system. Thirteen compounds including R_1, Rg_1, Re, Rf, Rg_2, Rb_1, Ro, Rb_2, Rb_3, Rd, (20*S*)-Rg_3, (20*R*)-Rg_3, Rk_2 in *P. ginseng* were identified by comparing their retention time with the reference standards displayed in Fig. 1B. The similarities of the entire chromatographic profiles of SJD and

Table 1
Precision, repeatability and stability of SJD samples.

Retention time (min)	Compound names	Precision (n = 5)RSD (%)	Repeatability (n = 5)RSD (%)	Stability (n = 5)RSD (%)
16.97	R_1	0.56	0.64	2.64
19.16	Rg_1	0.87	2.38	1.54
19.60	Re	0.64	1.12	0.92
28.73	Rf	0.57	1.07	0.71
31.49	Rg_2	0.24	1.63	2.23
32.30	Rb_1	0.46	0.75	1.33
33.98	Ro	0.96	0.46	0.63
35.98	Rb_2	0.75	0.84	1.95
36.61	Rb_3	1.26	1.37	1.84
40.13	Rd	0.74	1.73	0.73
43.64	20(S)-Rg_3	0.64	0.63	0.63
44.01	20(R)-Rg_3	0.63	0.42	1.74
52.60	Rk_2	0.06	0.21	0.93

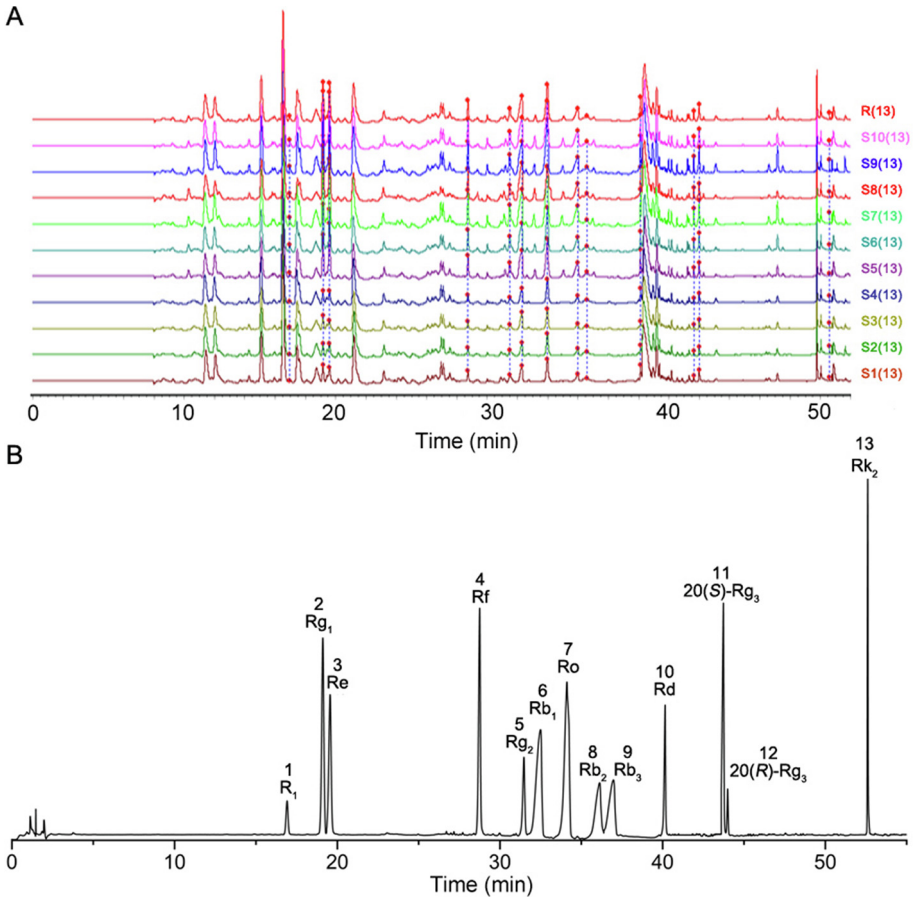

Fig. 1. UPLC chromatograms of SJD samples (A) and reference standards of *P. ginseng* (B). R: reference fingerprint.

the collected information of different batches of *P. ginseng* were shown in Table 2. The similarity degrees of 10 batches of SJD samples were above 0.97 which indicated that all the SJD samples were of good consistency. The relative peak areas of the above 13 common peaks were listed in Table S1 (Supplemental Table S1). The RSD values of 10 batches of SJD were all over 20%, which indicated that there were significant differences in ginsenoside content among different batches.

3.2. Results of anti-inflammatory experiments

Previous studies showed that weight loss, colon length, and diarrhea rectal bleeding were the indicators to evaluate the ulcerative colitis induced by DSS (Kim, Shajib, Manocha, & Khan, 2012; Nunes et al., 2019). As shown in Fig. 2A, the weight of mice in the control group gradually increased, while that of UC mice decreased obviously from the fourth day. After oral administration of SJD, the weight of UC mice in SJD groups (S1−S10) was gradually restored. The colon length of model group shown in Fig. 2B was significantly shorter than those of normal mice, which was one of the evidence of ulcerative colitis (Lee, Kwon, & Cho, 2018). In contrast with the UC model group, the length of colon in SJD group (S10) was ameliorated remarkably. From above, the increased body weight and colon length indicated good therapeutic effects of SJD on UC.

In order to observe the changes of colon tissue in control group, UC model group and SJD groups, sections of colon tissues were

Table 2
Collected information and similarity of samples.

Sample No.	Sources	Ages	Cultivation mode	Acquisition time	Similarity
S1	Heilongjiang	4	Farmland cultivation	May 2017	0.991
S2	Heilongjiang	4	Farmland cultivation	April 2017	0.978
S3	Jilin	4	Farmland cultivation	April 2017	0.988
S4	Jilin	4	Farmland cultivation	May 2017	0.984
S5	Jilin	4	Under forest	October 2018	0.994
S6	Jilin	5	Under forest	October 2018	0.997
S7	Jilin	6	Under forest	October 2018	0.993
S8	Jilin	15	Under forest	October 2018	0.976
S9	Jilin	4	Farmland cultivation	October 2018	0.997
S10	Jilin	5	Farmland cultivation	October 2018	0.999

stained with H&E (Fig. 3). In the control group, the structure of each layer of colon was clear, the mucosa epithelium was intact, and the glands were arranged regularly. While in the model group, the colonic submucosa edema, infiltration of inflammatory cells (neutrophils or macrophages) in the mucosa and submucosa, loss and destruction of crypts and atrophy of glands were observed. For the SJD group, the structure of each layer of colon was clear, the mucosa epithelium was complete and the arrangement of glands was regular. The results demonstrate that SJD could recover the loss of barrier function and tissue damage caused by UC.

Increasing evidence suggests that intestinal tight junction (TJ) proteins consisting of ZO-1 and occludin are key components of the intestinal mucosal barrier and participates in the development of UC (Perrier & Rutgeerts, 2011; Dokladny, Zuhl, & Moseley, 2016; Tan & Zheng, 2018). The effects of SJD on the expressions of occludin and ZO-1 in colons of mice of control and experimental groups were shown in Fig. 4. It is clear from the results that the amount of expression of occludin and ZO-1 in the model group both decreased markedly, while the expression in the UC mice was up-regulated under the treatment of SJD. This implies that SJD acted a protective effect on intestinal mucosal barrier by means of increasing the expression of TJ proteins.

Four proinflammatory cytokines including TNF-α, IL-1β, IL-6 and NO in the serum of each group were presented in Fig. 5. The levels of TNF-α, IL-1β, IL-6 and NO in the serum of UC model group were remarkably increased compared to the control group. Whereas, the SJD groups (S1 – S10) decreased the expression of inflammatory factors in varying degrees. Overall, these results indicated that SJD alleviated inflammatory response in DSS-induced UC mice.

3.3. Results of GRA with four pharmacodynamics indexes

TNF-α, IL-1β, NO and IL-6 related to inflammation were chosen to be four reference series and the 13 values of chromatogram peaks were regarded as compared series. The Grey relational coefficient between the compared and reference series was calculated with a resolution rate of 0.5. The Grey relational coefficient reflects the level of anti-inflammation. The higher the Grey relational coefficient, the greater the correlation between the compounds and the activity. According to the results exhibited in Fig. 6, the order of grey relational grade of the TNF-α was as follows: P1 > P9 > P5 > P7 > P4 > P13 > P8 > P2 > P6 > P3 > P12 > P11 > P10, the order of grey relational grade of the IL-1β was as follows: P1 > P9 > P5 > P4 > P13 > P8 > P7 > P3 > P12 > P6 > P11 > P2 > P10, the order of grey relational grade of the NO was as follows: P1 > P9 > P5 > P4 > P13 > P8 > P7 > P3 > P6 > P2 > P10 > P12 > P11, the order of grey relational grade of the IL-6 was as follows: P1 > P9 > P5 > P4 > P13 > P7 > P8 > P3 > P6 > P2 > P12 > P11 > P10. Following these results, we can conclude that the sequence above is coincident. P1 (R_1) was the highest influence to resist inflammation. P5 (Rg_2) and P9 (Rb_3) also showed a prominent influence to resist inflammation with the correlation degree in all reference series greater than 0.7. P2, P3, P4, P6, P7, P8, P13 possessed smaller power to resist inflammation, and P10, P11, P12 had a relatively fainter effect. Therefore, R_1 (P1), Rg_2 (P5) and Rb_3 (P9) were considered as key components to resisting inflammation due to their higher grey relational grade.

3.4. Verification experiment of anti-inflammatory activity

Macrophage inflammation also plays an important role in the course of the disease in the intestinal inflammation model (Lin et al., 2014; Chen et al., 2018), so we confirmed that anti-inflammatory effects of P1, P5 and P9 in the treatment of UC through detecting NO and TNF-α production in LPS-induced macrophage inflammation model. The results in Fig. 7 (A–C) illustrated that R_1, Rg_2 and Rb_3 could inhibit NO production and the anti-inflammatory activity showed dose-dependence. In addition, R_1, Rg_2 and Rb_3 were mixed in proportion to the corresponding

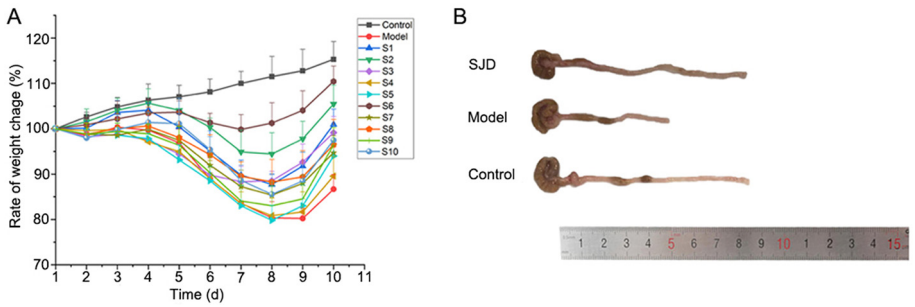

Fig. 2. SJD improved DSS-induced colitis in mice. (A) The rate of body weight changes of mice; (B) The colon length of mice in different groups.

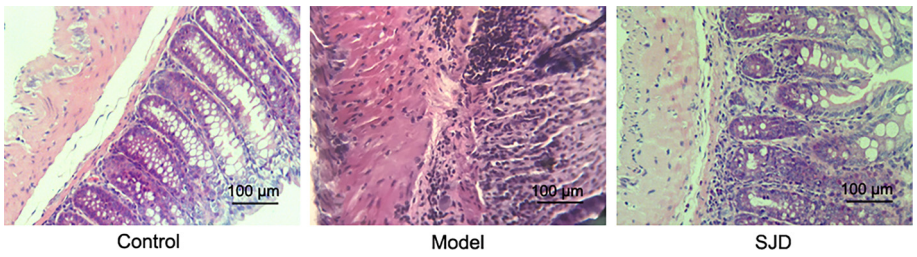

Fig. 3. Sections of colon tissues stained with H&E. (Magnification: ×400).

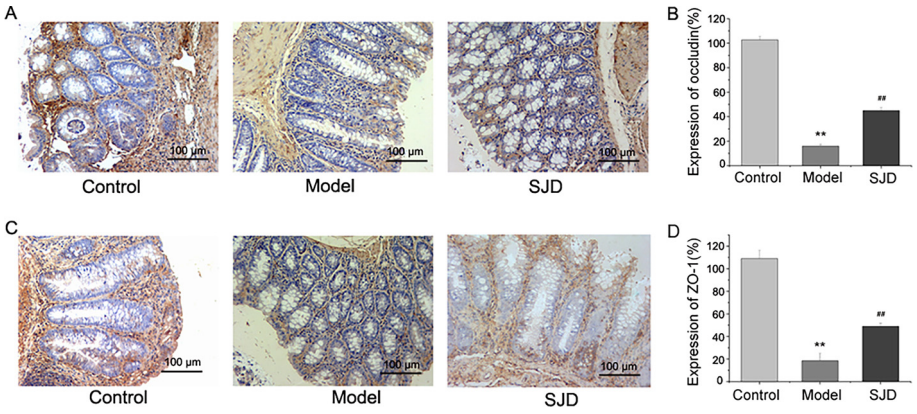

Fig. 4. Immunohistochemical expression of occludin (A) and ZO-1 (C) in colons. The expression of occludin and ZO-1 shown in (B) and (D) were calculated by the number of positive cells × intensity of positive cells. Data was analyzed by one-way ANOVA followed by post hoc Dunnett's test. $^{**}P < 0.01$ *vs* control group; $^{\#\#}P < 0.01$ *vs* model group.

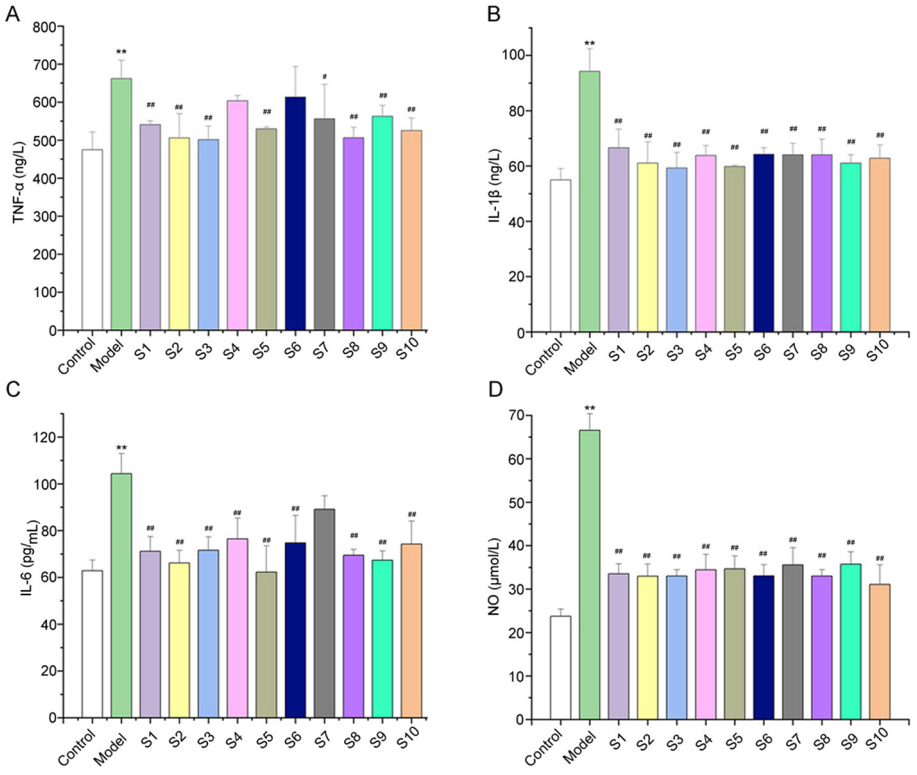

Fig. 5. Effects of SJD on levels of proinflammatory cytokines of TNF-α (A), IL-1β (B), IL-6 (C) and NO (D) in serum of UC mice. Data was analyzed by one-way ANOVA followed by post hoc Dunnett's test. $^{**}P < 0.01$ *vs* control group; $^{\#\#}P < 0.01$ *vs* model group.

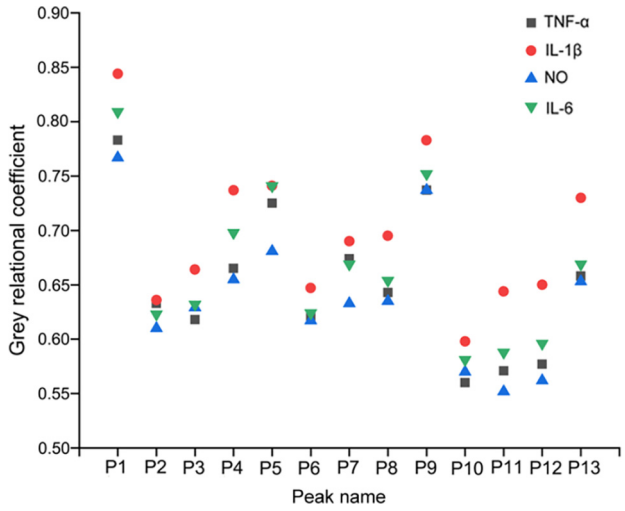

Fig. 6. Calculated grey relational coefficient of 13 chromatographic peaks correlated with anti-inflammatory activity deduced by GRA.

content in model SJD as a mixture (Supplemental Table S2 and S3) to compare with the inhibitory effects of SJD on NO production. It can be seen from Fig. 7 (D), the inhibition of NO production of the mixture was close to SJD which demonstrated that three compositions in *P. ginseng* might play important roles in the anti-inflammatory activity of SJD.

From Fig. 7(E–G), it was observed that R_1, Rg_2 and Rb_3 can inhibit the content of TNF-α in the LPS-induced macrophage and the inhibitory effect improved with the increase of concentration. The effect on the TNF-α in the mixture was quite close to SJD (Fig. 7H) which also pointed out that R_1, Rg_2 and Rb_3 were the main anti-inflammatory ingredients in SJD.

4. Discussion

P. ginseng is a traditional herbal drug widely applied clinically with abundant pharmacological activities. The composition of *P. ginseng* varies with plant species, geographical origin and age which caused different medicinal properties and economic value. The existing quality control methods are mainly concerned with the establishment of ginsenoside detection method which strips the association between medicinal ingredients and pharmacological actions (Cheng et al., 2021; Xu et al., 2021). They are insufficient to assess *P. ginseng* in the herbal markets and clinical raw materials selection of *P. ginseng*. Spectrum-effect relationship can integrate the chemical fingerprints and efficacy indicators to disclose the efficacy components of TCM. It is particularly suitable for quality control of complex herbal medicine systems. Therefore, the UPLC fingerprints of 10 batches of SJD (S1–S10) from different resources of *P. ginsengs* were established for exploring the spectrum-effect relationship. Precision, repeatability and sample stability in method validation are crucial aspects for the quality of results. RSD values showed that they were always <3% during the analysis. Therefore, the detection method exhibited good performance with high precision and repeatability, and the samples were stable in the detection conditions. Considering the characteristics of multiple effects of *P. ginseng*, it is more reliable to investigate the pharmacodynamic components in the context of clinical application. Therefore, SJD with *P. ginseng* as the sovereign drug was selected to recreate the therapeutic environment of *P. ginseng*.

SJD has a pharmacological effect on gastrointestinal function, immune system, ulcers, and tissue repair. It is often used clinically for peptic ulcers such as UC (Tian et al., 2021). UC, one of inflammatory bowel disease, is a chronic inflammatory state of the gastrointestinal tract. There is evidence that proinflammatory cytokines TNF-α, IL-1β, IL-6 and NO all are indispensable to the inflammatory response in the pathogenesis of UC (Dinarello, 2009; McAlindon, Hawkey, & Mahida, 1998; Li et al., 2010; Jahanshahi et al., 2004; Gillberg et al., 2012). In addition, TNF-α was confirmed to improve the expressions of IL-1β, IL-6 in UC (Clark, 2007; Sands & Kaplan, 2007; Bradley, 2008; Pugliese et al., 2017). For the sake of investigating the effective components of SJD in treating UC, the above four inflammatory factors were selected as effective indicators and correlated with the fingerprint of chemical components by GRA. It can be inferred that SJD reduced the expression of TNF-α, IL-1β, IL-6, NO and promoted the expressions of tight junction proteins such as occludin, and ZO-1 to maintain the intestinal mucosal barrier function for atten-

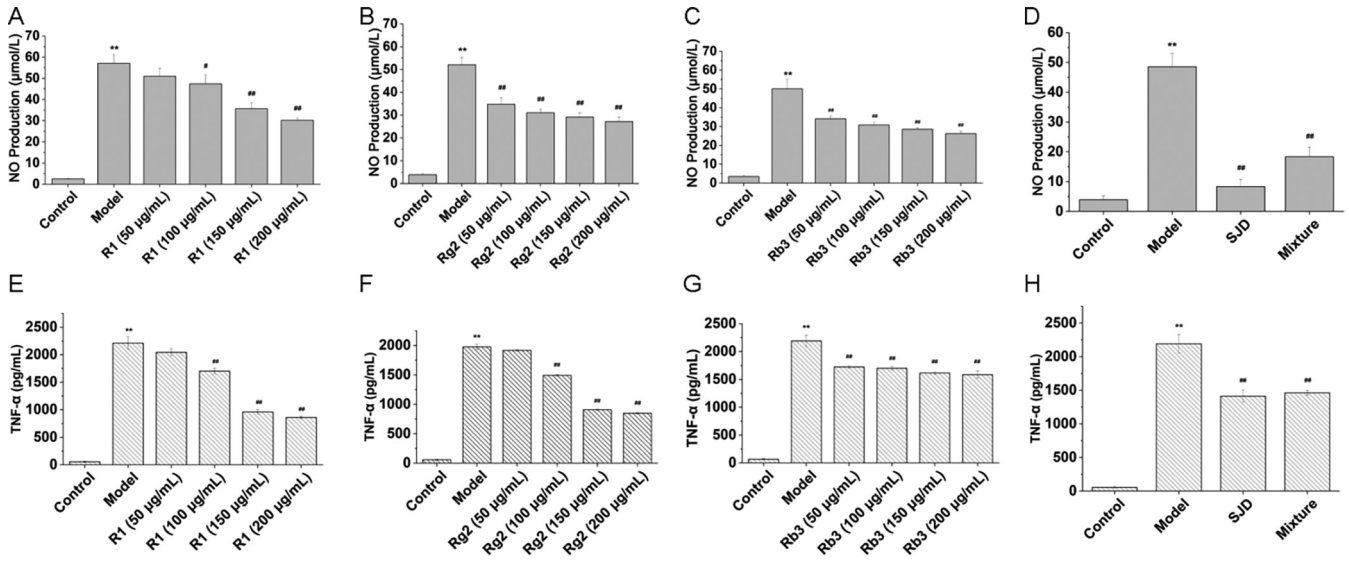

Fig. 7. Effects of R_1, Rg_2, Rb_3, SJD and mixture on levels of NO (A – D) and TNF-α (E–H) in macrophage. Data are expressed as mean ± SD for three independent experiments. Data was analyzed by one-way ANOVA followed by post hoc Dunnett's test. $^{**}P < 0.01$ *vs* control group; $^{\#}P < 0.05$, $^{\#\#}P < 0.01$ *vs* model group.

uating UC in mice. The anti-inflammatory effects of *P. ginseng* have been extensively studied and approven by purified ginsenosides (Chen, Rong, & Qiao, 2014; Agarwal, Nakara, & Shanmugam, 2019; Wang et al., 2018; Huynh, Baek, Sim, Myung, & Heo, 2020). In good agreement with previous results, GRA results indicate that R_1, Rg_2, Rb_3 might explain the anti-inflammatory effect of *P. ginseng* in SJD. Meanwhile, the above spectrum-effect relationship results illustrated that R_1, Rg_2, Rb_3 might be the main anti-inflammatory compounds in SJD. The anti-inflammatory activities of R_1, Rg_2, Rb_3 were confirmed through LPS-stimulated RAW264.7 murine macrophages cell.

The pharmacodynamic components filtrated by biological activity will promote the establishment of quality standards and the variety selection of *P. ginseng*. Recent studies have proven its benefits in screening the activities of anti-lung cancer and diabetic retinopathy in *P. ginseng* (Zhou, Liu, Zhang, Li, & Li, 2021; Yu et al., 2022). Due to the abundant pharmacological activity of *P. ginseng*, more quality control markers are still needed to be explored.

5. Conclusion

This study focused on providing chemical components highly correlated with pharmacodynamic indexes by spectrum-effect relationship. The fingerprints of 10 batches of SJD were built by UPLC. According to the results of pharmacological experiments, SJD has a significant therapeutic effect on UC. Grey relational coefficient of GRA revealed that R_1, Rg_2 and Rb_3 have the most significant effect on the anti-inflammatory action of *P. ginseng*. Therefore, the spectrum-effect relationship can be applicable for the detection of *P. ginseng*'s anti-inflammatory components in SJD.

Declaration of Competing Interest

The authors declare that they have no known competing financial interests or personal relationships that could have appeared to influence the work reported in this paper.

Acknowledgments

This study was financially supported by Science Foundation of Jilin Educational Committee (No. JJKH20200363KJ). Jilin Science & Technology Development Plan (No. 20190304009YY). Jilin Science & Technology Development Plan (No. 20200404090YY).

Appendix A. Supplementary data

Supplementary data to this article can be found online at https://doi.org/10.1016/j.chmed.2022.04.003.

References

Agarwal, H., Nakara, A., & Shanmugam, V. K. (2019). Anti-inflammatory mechanism of various metal and metal oxide nanoparticles synthesized using plant extracts: A review. *Biomedicine & Pharmacotherapy, 109*, 2561–2572.

Bradley, J. R. (2008). TNF-mediated inflammatory disease. *The Journal of Pathology, 214*(2), 149–160.

Cao, Y. Y., Li, S. H., Yuan, S., Zhang, Q. G., & Liu, L. P. (2021). Research progress on mechanism of antiarrhythmic action of *Panax ginseng*. *Chinese Traditional and Herbal Drugs, 52*(10), 3157–3166.

Chen, F., & Huang, G. L. (2019). Antioxidant activity of polysaccharides from different sources of ginseng. *International Journal of Biological Macromolecules, 125*, 906–908.

Chen, H., Shi, H. T., Liu, Y. P., Ren, X. Y., He, S. X., Chang, X. M., & Yin, Y. (2018). Activation of corticotropin-releasing factor receptor 1 aggravates dextran sodium sulphate-induced colitis in mice by promoting M1 macrophage polarization. *Molecular Medicine Reports, 17*(1), 234–242.

Chen, Y. Q., Rong, L., & Qiao, J. O. (2014). Anti-inflammatory effects of *Panax notoginseng* saponins ameliorate acute lung injury induced by oleic acid and lipopolysaccharide in rats. *Molecular Medicine Reports, 10*(3), 1400–1408.

Cheng, Q., Peng, S. H., Li, F. Y., Cui, P. D., Zhao, C. X., Yan, X. H., ... Li, Z. (2021). Quality distinguish of Red Ginseng from different origins by HPLC–ELSD/PDA combined with HPSEC–MALLS–RID, focus on the Sugar-Markers. *Separations, 8*(11), 198.

Clark, I. A. (2007). How TNF was recognized as a key mechanism of disease. *Cytokine & Growth Factor Reviews, 18*(3–4), 335–343.

Dai, J., Liu, X., & Hu, F. (2014). Research and application for grey relational analysis in multigranularity based on normality grey number. *The Scientific World Journal, 2014* 312645.

Dinarello, C. A. (2009). Interleukin-1beta and the autoinflammatory diseases. *The New England Journal of Medicine, 360*(23), 2467–2470.

Dokladny, K., Zuhl, M. N., Moseley, P. L. (2016). Intestinal epithelial barrier function and tight junction proteins with heat and exercise. *Journal of Applied Physiology, 120*(6), 692-701.

Gao, B. B., Peng, Y., & Li, X. B. (2018). Research progress on intestinal immunoregulation and mechanism of Sijunzi Decoction polysaccharide. *Chinese Traditional and Herbal Drugs, 49*(2), 462–467.

Gillberg, L., Varsanyi, M., Sjöström, M., Lördal, M., Lindholm, J., & Hellstrom, P. M. (2012). Nitric oxide pathway-related gene alterations in inflammatory bowel disease. *Scandinavian Journal of Gastroenterology, 47*(11), 1283–1297.

Guo, Y. L., Wu, X. X., Wu, Q., Lu, Y., Shi, J., & Chen, X. (2018). Dihydrotanshinone I, a natural product, ameliorates DSS-induced experimental ulcerative colitis in mice. *Toxicology and Applied Pharmacology, 344*, 35–45.

Hao, J. J., Hu, H. W. Y., Liu, J., Wang, X., Liu, X. Y., Wang, J. B., ... Xiao, X. H. (2019). Integrated metabolomics and network pharmacology study on immunoregulation mechanisms of *Panax ginseng* through macrophages. *Evidence-Based Complementary and Alternative Medicine, 2019*, 3630260.

He, M., & Zhou, Y. (2021). How to identify "Material basis–Quality markers" more accurately in Chinese herbal medicines from modern chromatography-mass spectrometry data-sets: Opportunities and challenges of chemometric tools. *Chinese Herbal Medicines, 13*(1), 2–16.

Huynh, D. T. N., Baek, N., Sim, S., Myung, C. S., & Heo, K. S. (2020). Minor ginsenoside Rg2 and Rh1 attenuates LPS-induced acute liver and kidney damages via downregulating activation of TLR4-STAT1 and inflammatory cytokine production in macrophages. *International Journal of Molecular Sciences, 21*(18), 6656.

Jahanshahi, G., Motavasel, V., Rezaie, A., Hashtroudi, A. A., Daryani, N. E., & Abdollahi, M. (2004). Alterations in antioxidant power and levels of epidermal growth factor and nitric oxide in saliva of patients with inflammatory bowel diseases. *Digestive Diseases and Sciences, 49*(11–12), 1752–1757.

Kadier, A., Abdeshahian, P., Simayi, Y., Ismail, M., Hamid, A. A., & Kalil, M. S. (2015). Grey relational analysis for comparative assessment of different cathode materials in microbial electrolysis cells. *Energy, 90*, 1556–1562.

Kang, J., Lee, S., Kang, S., Kwon, H. N., Park, J. H., Kwon, S. W., & Park, S. (2008). NMR-based metabolomics approach for the differentiation of ginseng (*Panax ginseng*) roots from different origins. *Archives of Pharmacal Research, 31*(3), 330–336.

Kim, J. J., Shajib, M. S., Manocha, M. M., & Khan, W. I. (2012). Investigating intestinal inflammation in DSS-induced model of IBD. *Jove-Journal of Visualized Experiments, 60*, e3678.

Lee, S. H., Kwon, J. E., & Cho, M. L. (2018). Immunological pathogenesis of inflammatory bowel disease. *Intestinal Research, 16*(1), 26–42.

Lee, Y. Y., Saba, E., Irfan, M., Kim, M., Chan, J. Y., Jeon, B. S., ... Rhee, M. H. (2019). The anti-inflammatory and anti-nociceptive effects of Korean black ginseng. *Phytomedicine, 54*, 169–181.

Li, S., Li, X. R., Wang, G. L., Nie, L. X., Yang, Y. J., Wu, H. Z., ... Lin, R. C. (2012). Rapid discrimination of Chinese red ginseng and Korean ginseng using an electronic nose coupled with chemometrics. *Journal of Pharmaceutical and Biomedical Analysis, 70*, 605–608.

Li, X. D., Chen, H. Y., Jia, W., & Xie, G. X. (2013). A metabolomics-based strategy for the quality control of traditional Chinese medicine: Shengmai injection as a case study. *Evidence-Based Complementary and Alternative Medicine, 2013* 836179.

Li, Y., de Haar, C., Chen, M., Deuring, J., Gerrits, M. M., Smits, R., ... van der Woude, C. J. (2010). Disease-related expression of the IL6/STAT3/SOCS3 signalling pathway in ulcerative colitis and ulcerative colitis-related carcinogenesis. *Gut, 59*(2), 227–235.

Lin, Y., Yang, X. G., Yue, W. J., Xu, X. F., Li, B. J., Zou, L. L., & He, R. (2014). Chemerin aggravates DSS-induced colitis by suppressing M2 macrophage polarization. *Cellular & Molecular Immunology, 11*(4), 355–366.

Liu, C. X., & Xiao, P. G. (1992). Recent advances on ginseng research in China. *Journal of Ethnopharmacology, 36*(1), 27–38.

Liu, H. Y., Zhu, S., Liu, Q., & Zhang, Y. Q. (2019). Spectrum-effect relationship study between HPLC fingerprints and antioxidant of honeysuckle extract. *Biomedical Chromatography, 33*(10), e4583.

Lu, Y., Lin, H. J., Zhang, J. W., Wei, J. A., Sun, J., & Han, L. (2017). Sijunzi Decoction attenuates 2, 4, 6-trinitrobenzene sulfonic acid (TNBS)-induced colitis in rats and ameliorates TNBS-induced claudin-2 damage via NF-κB pathway in Caco2 cells. *BMC Complementary and Alternative Medicine, 17*(1), 35.

McAlindon, M. E., Hawkey, C. J., & Mahida, Y. R. (1998). Expression of interleukin 1 beta and interleukin 1 beta converting enzyme by intestinal macrophages in health and inflammatory bowel disease. *Gut, 42*(2), 214–219.

Nelabhotla, D. M., Jayaraman, T. V., Asghar, K., & Das, D. (2016). The optimization of chemical mechanical planarization process-parameters of c-plane gallium-nitride using Taguchi method and grey relational analysis. *Materials & Design, 104*, 392–403.

Nunes, N. S., Chandran, P., Sundby, M., Visioli, F., Gonçalves, F., Burks, S. R., ... Frank, J. A. (2019). Therapeutic ultrasound attenuates DSS-induced colitis through the cholinergic anti-inflammatory pathway. *EBioMedicine, 45*, 495–510.

Perrier, C., & Rutgeerts, P. (2011). Cytokine blockade in inflammatory bowel diseases. *Immunotherapy, 3*(11), 1341–1352.

Pugliese, D., Felice, C., Papa, A., Gasbarrini, A., Rapaccini, G. L., Guidi, L., & Armuzzi, A. (2017). Anti TNF-α therapy for ulcerative colitis: Current status and prospects for the future. *Expert Review of Clinical Immunology, 13*(3), 223–233.

Qiao, C., Wan, J., Zhang, L., Luo, B., Liu, P. L., Di, A., ... Zhao, G. (2019). Astragaloside II alleviates the symptoms of experimental ulcerative colitis *in vitro* and *in vivo*. *American Journal of Translational Research, 11*(11), 7074–7083.

Sands, B. E., & Kaplan, G. G. (2007). The role of TNFalpha in ulcerative colitis. *Journal of Clinical Pharmacology, 47*(8), 930–941.

Shan, S. M., Luo, J. G., Huang, F., & Kong, L. Y. (2014). Chemical characteristics combined with bioactivity for comprehensive evaluation of *Panax ginseng* C.A. Meyer in different ages and seasons based on HPLC-DAD and chemometric methods. *Journal of Pharmaceutical and Biomedical Analysis, 89*, 76–82.

Shen, C. H., Liu, C. T., Song, X. J., Zeng, W. Y., Lu, X. Y., Zheng, Z. L., ... Yan, P. (2018). Evaluation of analgesic and anti-inflammatory activities of *Rubia cordifolia* L. by spectrum-effect relationships. *Journal of Chromatography B, 1090*, 73–80.

Shi, W., Wang, Y. T., Li, J., Zhang, H. Q., & Ding, L. (2007). Investigation of ginsenosides in different parts and ages of *Panax ginseng*. *Food Chemistry, 102*(3), 664–668.

Song, H. P., Li, R. Y., Huang, H. Y., Cai, X., Yuan, Z. Y., Liu, P. A., & Zhou, C. (2016). Sijunzi Decoction promote the repair of intestinal epithelial cell injury via activating TLR-2/My D88 signaling pathway. *Journal of Chinese Medicinal Materials, 39*(9), 2081–2085.

Tan, Y., & Zheng, C. Q. (2018). Effects of alpinetin on intestinal barrier function, inflammation and oxidative stress in dextran sulfate sodium-induced ulcerative colitis mice. *American Journal of the Medical Sciences, 355*(4), 377–386.

Tian, S. W., Zhang, Y. L., Wang, B., Liu, J. P., Wang, C., & Zhang, J. (2021). Clinical efficacy and safety of modified Sijunzi decoction for the treatment of ulcerative colitis. *Medicine, 100*(4), e23703.

Wang, M. Y., Chen, X. N., Jin, W. Q., Xu, X. H., Li, X. Y., & Sun, L. W. (2018). Ginsenoside Rb3 exerts protective properties against cigarette smoke extract-induced cell injury by inhibiting the p38 MAPK/NF-kappaB and TGF-beta1/VEGF pathways in fibroblasts and epithelial cells. *Biomedicine & Pharmacotherapy, 108*, 1751–1758.

Wang, Y. Y., He, S., Cheng, X. C., Lu, Y. X., Zou, Y. P., & Zhang, Q. L. (2013). UPLC–Q-TOF-MS/MS fingerprinting of traditional Chinese formula SiJunZiTang. *Journal of Pharmaceutical and Biomedical Analysis, 80*, 24–33.

Xie, P. S., Chen, S. B., Liang, Y. Z., Wang, X. H., Tian, R. T., & Upton, R. (2006). Chromatographic fingerprint analysis–a rational approach for quality assessment of traditional Chinese herbal medicine. *Journal of Chromatography A, 1112*(1–2), 171–180.

Xu, X. Y., Wang, S. M., Wang, H. M., Hu, W. D., Han, L. F., Chen, B. X., ... Yang, W. Z. (2021). Simultaneous quantitative assays of 15 ginsenosides from 119 batches of ginseng samples representing 12 traditional Chinese medicines by ultra-high performance liquid chromatography coupled with charged aerosol detector. *Journal of Chromatography A, 1655*(11) 462504.

Yu, W. G., Lu, B., Zhang, H. W., Zhang, Y. X., & Yan, J. (2016). Effects of the Sijunzi decoction on the immunological function in rats with dextran sulfate-induced ulcerative colitis. *Biomedical Reports, 5*(1), 83–86.

Yu, Y. T., Zhu, Z. Y., Xie, M. J., Deng, L. P., Xie, X. J., & Zhang, M. (2022). Investigation on the Q-markers of Bushen Huoxue Prescriptions for DR treatment based on chemometric methods and spectrum-effect relationship. *Journal of Ethnopharmacology, 285* 114800.

Zhang, J. D., Chen, T., Li, K., Xu, H. Y., Liang, R. X., Wang, W. H., ... Yang, B. (2019). Screening active ingredients of rosemary based on spectrum-effect relationships between UPLC fingerprint and vasorelaxant activity using three chemometrics. *Journal of Chromatography B, 1134–1135* 121854.

Zhang, T., Han, M., Yang, L. M., Han, Z. M., Cheng, L., Sun, Z., & Yang, L. (2018). The effects of environmental factors on ginsenoside biosynthetic enzyme gene expression and saponin abundance. *Molecules, 24*(1), 14.

Zhou, S., Zhou, L. W., Yu, L. T., Liu, S. C., Luo, Q. M., Sun, P. J., & Wu, J. K. (2016). Monitoring chip fatigue in an IGBT module based on grey relational analysis. *Microelectronics Reliability, 56*, 49–52.

Zhou, X. W., Liu, H. Y., Zhang, M. Y., Li, C. Y., & Li, G. H. (2021). Spectrum-effect relationship between UPLC fingerprints and anti-lung cancer effect of *Panax ginseng*. *Phytochemical Analysis, 32*, 339–346.